HHS Public Access

Author manuscript

Ultrasound Med Biol. Author manuscript; available in PMC 2016 August 01.

Published in final edited form as:

Ultrasound Med Biol. 2015 August ; 41(8): 2191–2201. doi:10.1016/j.ultrasmedbio.2015.04.002.

Acoustic cavitation-mediated delivery of small interfering ribonucleic acids with phase-shift nanoemulsions

Mark T. Burgess[1,3] and **Tyrone M. Porter**[1,2,3]

[1]Department of Mechanical Engineering, Boston University, Boston, MA

[2]Department of Biomedical Engineering, Boston University, Boston, MA

[3]Center for Nanoscience and Nanobiotechnology, Boston University, Boston, MA

Abstract

Localized, targeted delivery of small interfering ribonucleic acid (siRNA) has been the foremost hurdle in the use of siRNA for the treatment of various diseases. Major advances have been achieved in the synthesis of siRNA, which has led to greater target messenger RNA (mRNA) silencing and stability in physiological conditions. Although numerous delivery strategies have shown promise, there are still limited options for targeted delivery and release of siRNA administered systemically. In this *in vitro* study, phase-shift nanoemulsions (PSNE) were explored as cavitation nuclei to facilitate free siRNA delivery to cancer cells via sonoporation. A cell suspension containing varying amounts of PSNE and siRNA was exposed to 5 MHz pulsed ultrasound at fixed settings (6.2 MPa peak negative pressure, 5 cycle pulses, 250 Hz pulse repetition frequency, and total exposure duration of 100 seconds). Inertial cavitation emissions were detected throughout the exposure using a passive cavitation detector. Successful siRNA delivery was achieved (*i.e.* > 50% cell uptake) with high viability (> 80% viability). The percentage of cells with siRNA uptake was correlated with the amount of inertial cavitation activity generated from vaporized PSNE. The siRNA remained functional after delivery, significantly reducing expression of green fluorescent protein (GFP) in a stably transfected cell line. These results show that vaporized PSNE can facilitate siRNA entry into the cytosol of a majority of sonicated cells and may provide a non-endosomal route for siRNA delivery.

Keywords

siRNA; acoustic cavitation; sonoporation; microbubbles; phase-shift nanoemulsions; ultrasound; acoustic droplet vaporization; nanomedicine

Corresponding Author: Mark T. Burgess, Department of Mechanical Engineering, 110 Cummington Mall, Boston, MA, 02215. marktb@bu.edu.

Introduction

RNA interference (RNAi) based therapeutics are in development for numerous diseases including cancer, viral infections, and other genetic disorders (Davidson and McCray 2011). These double stranded RNA molecules allow post-transcriptional modification of gene expression with remarkable potency and specificity (Vaishnaw et al. 2010). In particular, small interfering RNAs (siRNA) have attracted much interest for their ability to knockdown specific proteins central to disease progression (Lares et al. 2010). Once introduced into the cytosol of cells, siRNA molecules are incorporated into the RNAi pathway where they lead to degradation of complementary messenger RNA (mRNA) molecules, which in turn leads to a reduction in targeted protein expression (Elbashir et al. 2001). In theory, this opens up the possibility of targeting any of the approximately 20,000 genes in the human genome with synthetic siRNA molecules. Proteins once considered undruggable using conventional small molecules can now be targeted, which could have a profound impact on the treatment of human diseases (Wu et al. 2014).

Effective siRNA delivery has remained an elusive challenge in the pursuit of its use as a systemically administered therapeutic. Small interfering RNA is large (~14 kDa), highly anionic, susceptible to enzymatic degradation, and rapidly filtered from circulation by the kidneys (Tokatlian and Segura 2010). Progress has been made in improving the pharmacokinetic properties of siRNA therapeutics through chemical modifications to the siRNA molecule and packaging into nanoparticles (Zhang et al. 2007; Behlke 2008; Whitehead et al. 2009). Numerous lipid and polymer based nanoparticles are currently being developed for siRNA delivery with a few under clinical trials (Burnett et al. 2011). These nanoparticles extend the half-life of siRNA in circulation and protect against degradation en route to diseased tissue. In regards to cancer therapies, nanoparticles are able to accumulate in tumors through the enhanced permeability and retention (EPR) effect (Fang et al. 2011). Nanoparticles are then internalized by cells through endosomal pathways, where endosomal escape must occur in order to release siRNA into the cytosol where it can access RNAi machinery. A recent article by Gilleron *et al.* (2013) showed that endosomal escape of siRNA happens at low efficiencies (1–2%) with lipid-based nanoparticle delivery. Therefore, it may be beneficial to bypass the endosomal pathways and deliver siRNA directly into the cell's cytosol.

Sonoporation, or the use of acoustic cavitation for cell membrane disruption, has been shown to facilitate non-endosomal delivery of large biomolecules such as drugs and genetic material into the cell cytosol (Lentacker et al. 2013). Acoustic cavitation can generate stresses on biological structures in close proximity due to microstreaming, bubble expansion/collapse, shockwave emission, and microjetting (Sundaram et al. 2003; Ohl et al. 2006; van Wamel et al. 2006; Wu and Nyborg 2008; Kooiman et al. 2011; Fan et al. 2012; Zhou et al. 2012). Gas-filled ultrasound contrast agents (UCAs) used for diagnostic imaging are typically employed as cavitation nuclei to induce these stresses for enhancement of gene and drug delivery (Ferrara et al. 2007; Sirsi and Borden 2012). Kinoshita *et al.* (2005) highlighted the possibility of using UCAs for intracellular delivery of siRNA and other studies have since shown promising results (Negishi et al. 2008). However, UCAs are limited to the vascular system due to their size (1–10 μm) and are quickly cleared from

circulation within minutes of injection by the mononuclear phagocyte system (MPS) and dissolution (Unger et al. 2004; Garg et al. 2013). Therefore, researchers have begun to explore submicron cavitation nuclei for ultrasound-mediated gene delivery to solid tumors (Suzuki et al. 2011; Endo-Takahashi et al. 2012).

Phase-shift nanoemulsions (PSNE) present an attractive alternative to UCAs for gene and drug delivery to solid tumors. PSNE are superheated nanodroplets of liquid perfluorocarbon that are stabilized with a biocompatible lipid, polymer, or protein shell. Ultrasound can be used to vaporize the perfluorocarbon core and the pressure threshold for vaporization depends upon numerous factors including the boiling point of the perfluorocarbon (Kawabata et al. 2005; Sheeran et al. 2012), ambient temperature (Fabiilli et al. 2009; Zhang and Porter 2010), ultrasound frequency (Kripfgans et al. 2000), and size of the droplet (Kripfgans et al. 2004; Fabiilli et al. 2009). In theory, PSNE vaporization could allow controlled initiation of acoustic cavitation in tissue where bubbles are difficult to form and control (Kopechek et al. 2013). PSNE combine the improved biocompatibility, long circulation, and extravasation properties of lipid-based nanoparticles with the beneficial bioeffects of acoustic cavitation, such as sonoporation. This unique class of emulsion has been utilized for drug delivery applications (Rapoport et al. 2009; Adan et al. 2012; Wang et al. 2012), contrast-enhanced ultrasound imaging (Sheeran et al. 2013b; Williams et al. 2013), and bubble-enhanced heating for high intensity focused ultrasound (HIFU) ablation (Kopechek et al. 2013; Phillips et al. 2013).

The objective of this study was to investigate the potential of PSNE as cavitation nuclei for delivery of free siRNA to *in vitro* cell suspensions. We hypothesize that vaporized PSNE can be used to transiently disrupt cell membranes in a manner similar to traditional UCAs and facilitate entry of siRNA into the cell cytoplasm. Therefore, we first examined the uptake of fluorescently tagged siRNA as a function of PSNE concentration. Cell suspensions containing siRNA and PSNE were exposed to short bursts of ultrasound with simultaneous detection of acoustic cavitation emissions. Cells were analyzed using flow cytometry and the correlation between siRNA uptake and acoustic cavitation activity was assessed. The second part of the study explored the delivery of siRNA designed to knockdown green florescent protein (GFP) in stably transfected cells. The PSNE concentration that yielded the highest uptake of siRNA was used along with varying doses of GFP targeted siRNA. The following sections outline the methodology used for PSNE fabrication, ultrasound experiments, and analysis. Finally, the results from the siRNA delivery experiments are discussed along with its implications for localized siRNA delivery using PSNE.

Materials and Methods

Nanoemulsion Preparation

Lipid coated perfluorocarbon nanoemulsions were prepared using a three step hydration, emulsification, and extrusion procedure (Kopechek et al. 2012). The lipids 1,2-dipalmitoyl-sn-glycero-3-phosphocholine (DPPC) and 1,2-dipalmitoyl-sn-glycero-3-phosphoethanolamine-N-[methoxy(polyethylene glycol)-2000] (DPPE-PEG2000) (Avanti Polar Lipids, Alabaster, AL, USA) were weighed and dissolved in chloroform (Sigma-Aldrich, St. Louis, MO, USA) at a molar ratio of 9:1 (DPPC:DPPE-PEG2000). A thin lipid

film was formed in a glass vial by evaporating the chloroform with a steady stream of argon. The vial was placed under vacuum overnight to remove any residual chloroform. Subsequently, the lipid film was hydrated for 1–2 hours at 50°C with phosphate buffered saline (PBS) (Boston Bioproducts, Ashland, MA, USA) with periodic vortexing and sonication in an ultrasonic bath (Cole-Parmer, Vernon Hills, IL, USA). The lipid vesicles were then sonicated using a high power sonication tip (Sonic & Materials, Newtown, CT, USA) for 1 minute to produce a clear solution of small lipid vesicles at a lipid concentration of 1 mg/mL.

Submicron perfluorocarbon emulsions were made by adding 100 μL of dodecafluoropentane (DDFP, 29°C boiling point) (FluoroMed, L.P., Round Rock, Texas, USA) to 3 mL of lipid solution and sonicating with a high power sonication tip in an ice water bath. A pulsing regime was used, 10 seconds ON, 50 seconds OFF, for a total ON time of 1 minute to prevent heating and vaporization of DDFP. This opaque suspension was then added to 7 mL of PBS and extruded 10 times through two stacked 200 nm polycarbonate filters using a LIPEX™ Extruder (Northern Lipids Inc., Burnaby, British Columbia). Excess lipid vesicles were removed by three centrifugal washes for 5 minutes at 3,000 *g*. Each time the PSNE pellet was resuspended with PBS.

Particle Sizing and Concentration

Tunable resistive pulse sensing (TRPS) with the qNano (Izon Science Ltd., Christchurch, New Zealand) was used to determine the size and concentration of PSNE. The qNano allows particle-by-particle counting and sizing of submicron particles as they pass through a stretchable nanopore. A NP200 nanopore (diameter range: 100 – 400 nm) was used along with 200 nm carboxylated polystyrene standards of known size and concentration for calibration. The PSNE were diluted a thousand-fold in PBS and at least 1000 nanopore blockade events were recorded at three different pressure driven flow regimes according to the manufacturer's instructions. This was repeated with 200 nm standards using the same instrument settings to determine the size and concentration of PSNE.

Ultrasound Set-up and Parameters

A 5-MHz spherically focused transducer (SU-108, Sonic Concepts, Bothell, Washington, USA) was submerged in a 37°C water bath and used to sonicate a cell suspension containing siRNA and PSNE (Figure 1). A 1.5 mL polypropylene microcentrifuge tube was used to house the cell suspension and was partially submerged in the water bath to allow propagation of the ultrasound into the suspension. According to the manufacturer's specifications, the focus of the transducer had a full-width half-maximum (FWHM) beamwidth of 0.32 mm and FWHM depth of 3 mm. The transducer was driven using a 55-dB RF amplifier (Electronics & Innovation, Rochester, NY, USA) and waveform generator (Agilent Technologies Inc., Santa Clara, CA, USA). The peak pressure output of the transducer at the focus was determined with a calibrated 75-μm needle hydrophone (Precision Acoustics, Dorchester, Dorset, England) positioned behind the wall of the microcentrifuge tube to account for attenuation. Pressure measurements were made up to 4 MPa (peak negative pressure) and then the data was extrapolated out to higher pressures using a linear fit of data between 2 MPa and 4 MPa peak negative pressure.

A passive cavitation detection scheme similar to the previous study by Zhang and Porter (2010) was employed for monitoring PSNE vaporization and inertial cavitation activity. A 2.25 MHz unfocused transducer (Olympus NDT Inc., Waltham, MA, USA) aligned perpendicular to the 5-MHz transducer (Figure 1) was operated as a passive cavitation detector (PCD), monitoring for acoustic emissions radiated during PSNE vaporization and subsequent inertial bubble collapse. The signal from the PCD was routed through a 2 MHz narrowband filter (FL= 1.6 MHz, FU= 2.2 MHz, Allen Avionics Inc., Mineola, New York, USA), amplified by 30 dB (Model DHPVA-100, Femto, Berlin, Germany), and digitized using a 14-bit oscilloscope board (GaGe Corp., Lockport, IN, USA) at a sampling rate of 50 MS/s. During each exposure at various PSNE concentrations, the PCD was triggered to acquire data upon every ultrasound pulse resulting in 25,000 individual traces. The data from all exposures was saved and post-processed using MATLAB (Mathworks, Natick, MA, USA) to quantify acoustic cavitation activity as shown in Figure 2. Each trace was gated in the time domain and the root mean squared (RMS) value was computed. The RMS values were then summated for each exposure and normalized to the exposure with the highest amount of cavitation activity. The mean and standard deviations of the normalized values were taken at each PSNE concentration (n=3) to provide a measure of the amount of cavitation activity for comparison with siRNA uptake and cell viability.

A series of preliminary studies were conducted to identify the acoustic pressure, pulse length, and pulse repetition frequency to be used in combination with PSNE for facilitating siRNA delivery to cells. We first identified the pressure threshold for PSNE vaporization using the method documented by Zhang and Porter (2010). Briefly, PSNE suspensions were sonicated with 5 cycle pulses and the peak negative pressure was increased (starting from 2 MPa) until the amplitude of the PCD trace increased by more than a factor of ten above baseline. Figure 2A illustrates the increased signal amplitude when above the vaporization threshold (peak negative pressure = 6.2 MPa) as compared to below. Next, PSNE were suspended with 250,000 human breast cancer cells in 25 μl of PBS and vaporized with HIFU (peak negative pressure = 6.2 MPa) and varying pulse length (5, 7, and 9 cycles at a 250 Hz pulse repetition frequency) and pulse repetition frequency (5 cycle pulse at 250, 500, and 1000 Hz). An MTT cell proliferation assay (ATCC, Manassas, VA, USA) was used to assess cell viability after treatment and the pulse length and pulse repetition frequency (PRF) that were the least lethal were used in subsequent sonoporation studies.

Small interfering RNA Delivery

Human breast adenocarcinoma cells (MDA-MB-231) were used in tests of fluorescent siRNA delivery while MDA-MB-231 cells stably expressing green fluorescent protein (GFP) were used in tests of functional siRNA delivery. Prior to ultrasound experiments, cells were grown to confluence in 75 cm^2 tissue cultured flasks and harvested using trypsin. Cells were counted using a hemacytometer and resuspended in serum free growth media at a concentration of 2.5×10^7 cells/mL. Aliquots of 10 μL were added to 1.5 mL polypropylene microcentrifuge tubes and placed in a 37°C water bath until the treatment.

Fluorescently tagged siRNA (siGLO green, GE Dharmacon, Lafayette, CO, USA) was suspended in PBS at a molar concentration of 50 μM. For each treatment, the cell suspension

was mixed with 5 μL of siGLO and 10 μL of a stock PSNE solution to give a final volume of 25 μL with a molar concentration of 10 μM siGLO and PSNE concentrations of 5×10^6, 1×10^7, 2.5×10^7, 5×10^7, 1×10^8, 2.5×10^8, 5×10^8 or 1×10^9 PSNE/mL. The focus of the 5 MHz transducer was positioned inside the cell suspension using a three-axis translation stage system (ThorLabs Inc., Newton, New Jersey, USA) and the suspension was immediately exposed to ultrasound (5 cycles, peak negative pressure = 6.2 MPa, PRF = 250 Hz, 100 second exposure) with a total of three exposures at each PSNE concentration.

Knockdown experiments were performed using similar experimental parameters except GFP targeted siRNA (GFP duplex I, GE Dharmacon, Lafayette, CO, USA) was used at molar concentrations of 0.1, 1.0, and 10 μM. PSNE were fixed at a concentration of 1×10^9 PSNE/mL and cells at a concentration of 10^7 cells/mL. Control groups using no siRNA (blank PBS) and non-targeting siRNA (siGENOME Non-targeting siRNA 2, GE Dharmacon, Lafayette, CO, USA) were also exposed to ultrasound. After the ultrasound exposures, cells were washed and incubated in 25 cm^2 tissue culture flasks for 48 hours before analysis of GFP knockdown. Knockdown experiments were also performed with a commercially available transfection agent (DharmaFECT 4, GE Dharmacon, Lafayette, CO, USA) according to the company's protocol. Briefly, cells were seeded onto 12 well plates at 50,000 cells per well and allowed to adhere overnight. Transfections were performed the following day using GFP targeted and non-targeted siRNA at molar concentrations of 50 nM (1 mL total volume in each well). The growth media was replaced after 24 hours and cells were harvested for analysis at 48 hours.

Analysis

For evaluation of ultrasound-mediated delivery of fluorescently tagged siRNA, cells were washed and resuspended in 250 μL of cold PBS (10^6 cells/mL) within 30 minutes of the ultrasound exposure. Propidium iodide (PI) was added at a concentration of 4 μg/mL to stain cells that had irreparable damage to the cell membrane during ultrasound exposure and therefore were defined as non-viable. The fraction of cells with intracellular siRNA and/or stained with propidium iodide were quantified using flow cytometry (FACSCalibur, BD Biosciences, San Jose, CA, USA). Assuming the flow cytometer operates at a constant flow rate, data was collected for one minute for comparison of the total number of cells counted between control and treatment groups to assure that no significant cell fragmentation or lysis had occurred during the treatment. Viable cells showing uptake were gated on the FL1 (siRNA) vs. FL3 (PI) scatter plot to eliminate non-viable cells during analysis of siRNA delivery. Uptake was defined as the percentage of cells above a certain threshold fluorescent intensity. The mean percentage of cells above the threshold for the control group was subtracted from each individual treatment at varying PSNE concentrations. Viability was defined in a similar manner using PI fluorescence, by subtracting the mean value of the control group from each individual treatment at varying PSNE concentrations. Qualitative analysis of siRNA uptake was performed by plating treated cells on 35 mm glass bottom dishes (MatTek Corporation, Ashland, MA, USA) for imaging with fluorescent microscopy (IX81, Olympus America Inc., Melville, NY, USA) eight hours after ultrasound exposure.

Cells treated with GFP targeted siRNA were harvested at 48 hours for analysis with flow cytometry. GFP knockdown was quantified by comparing the mean fluorescent intensity of the entire treated cell populations to that of the control populations, which was defined as a percent reduction in GFP fluorescent intensity. A second metric of cell viability was performed after delivery of GFP targeted siRNA using a cell proliferation assay (MTT Cell Proliferation Assay, ATCC, Manassas, VA, USA). The assay was used to quantify and compare cell proliferation between treated and control cell populations. Given that cell proliferation requires viable and functional cells, this assay allows for capturing acute and chronic effects of ultrasound and acoustic cavitation on cell viability.

Results

Particle Sizing and Concentration

The measured size distribution of the PSNE using the qNano is shown in Figure 3. The emulsification followed by extrusion technique produced a fairly narrow size distribution with a mean diameter of 213 nm (31.4 nm standard deviation) and a bulk concentration of 2.0×10^{11} PSNE/mL. The modal diameter was 203 nm (+/− 2.2 nm) with 10% of the population below 180.1 nm (d_{10} = 180.1), 90% of the population below 250.4 nm (d_{90} = 250.4).

Fluorescent siRNA delivery

The dependence of cell viability on pulse length and pulse repetition frequency (PRF) is shown in Figure 4. Varying pulse lengths (5, 7, and 9 cycles) at a fixed PRF (250 Hz) and varying PRFs (250, 500, and 1000 Hz) at a fixed number of cycles (5 cycles) were used to explore the relationship. An overall decrease in cell viability can be seen with increasing pulse lengths and PRFs. Significant differences relative to the ultrasound parameters used for siRNA delivery (5 cycles, 250 Hz PRF) can be seen at the highest pulse lengths and PRFs.

The use of a fluorescently tagged siRNA allowed assessment of siRNA uptake with flow cytometry and fluorescent microscopy. Figure 5 displays representative fluorescent microscopy and flow cytometry results. A large majority of the cells show uptake of siRNA, which was tagged with a green fluorophore. This specific siRNA molecule was designed to avoid RNAi machinery and localize to the nucleus over 24 hours. After eight hours a large majority of the siRNA appears to be diffuse in the cytosol of the cells and not localized to endosomes or cell nuclei.

Representative histograms of the flow cytometer results at different PSNE concentrations (1×10^9, 1×10^8, and 1×10^7 PSNE/mL) are also shown in Figure 5C–E. Two distinct cell populations emerged after ultrasound exposure showing high uptake or no uptake at all. There also exists some heterogeneity in uptake, with subpopulations of cells outside and in between the two distinct cell populations. This is consistent with previous sonoporation studies, which showed a similar heterogeneity in regards to uptake (Guzman et al. 2001; Sundaram et al. 2003). Three runs at different PSNE concentrations were performed and the quantitative results of siRNA uptake and cell viability are shown in Figure 6. The percent of

cells with siRNA uptake and percent of viable cells both had logarithmic trends that plateaued with increasing amounts of PSNE. There was no significant difference between treated and control groups in terms of the total number of cells counted by the flow cytometer.

Passive cavitation detection during the ultrasound treatments revealed a strong dependence on PSNE concentration with the amplitude and duration of cavitation activity. Figure 7A–D shows representative plots of the RMS amplitude of the PCD signal versus exposure duration at various PSNE concentrations (1×10^9 PSNE/mL, 1×10^8 PSNE/mL, 1×10^7 PSNE/mL, and no PSNE). The percentage of cells with siRNA uptake was correlated with the relative amount of cavitation activity as shown in Figure 8. The mean amount of cavitation activity was plotted against the mean uptake for each treatment group. Uptake and cavitation activity both had logarithmic trends that plateaued with increasing concentrations of PSNE (Figures 7E & 6). A linear relationship between cavitation activity and uptake was seen in Figure 8, with no significant changes in uptake at the highest levels of cavitation activity. The percentage of viable cells on the other hand had a weak correlation with cavitation activity as shown in Figure 8. A slight decrease in cell viability can be seen with increasing amounts of cavitation activity.

GFP Knockdown

Functional siRNA experiments were performed with siRNA designed to knockdown GFP. The flow cytometer histograms in Figure 9A–B show an overall shift to the left for treated cells, indicating a reduction in the amount of GFP produced by cells that survived the ultrasound exposure. Only a fraction of the cells showed a reduction in GFP with treatments using PSNE (Figure 9A), while the entire cell population showed a decrease with the commercial transfection agent (Figure 9B). This may be explained by the distinct populations of cells showing uptake or no uptake as observed with fluorescent siRNA delivery (Figure 5), therefore leading to heterogeneity in GFP reduction. The bar plots in Figure 9C show the percent reduction in GFP fluorescent intensity for respective treatment and control groups. All concentrations of GFP siRNA (10 μM, 1 μM, and 0.1 μM) resulted in a 40–50% reduction in GFP intensity, which was comparable to knockdown achieved with siRNA delivered via a commercial transfection agent (54 +/− 0.7% reduction).

Discussion

The strategies for siRNA delivery have largely been based upon nanoparticle carriers that suffer from toxicity issues, poor uptake by desired cells, and inefficient endosomal escape and release of siRNA to the target area (Wu et al. 2014). PSNE in combination with focused ultrasound technologies may provide a way to localize and control the release and delivery of siRNA therapeutics. Sonoporation has previously been offered as an option for *in vitro* siRNA delivery. Unfortunately, sonoporation has shown limited efficiency for intracellular delivery of a broad spectrum of biomolecules (Liu et al. 2012). The current study was motivated by the need to resolve this limitation in order to enable development of an alternative delivery method for siRNA therapeutics.

From a mechanistic perspective, sonoporation is made possible by acoustic cavitation. Expanding and compressing/collapsing microbubbles near cells can cause stresses that act to disrupt cell membranes temporarily or permanently, resulting in either viable or non-viable sonoporated cells, respectively. The microbubble activity can be violent or gentle depending on the type of cavitation. Stable cavitation is defined by repetitive oscillations around some equilibrium size, while inertial cavitation is defined by explosive growth and collapse of microbubbles (Neppiras 1980; Leighton 1994). High-speed optical microscopy during the vaporization of submicron nanoemulsions has shown that vaporization occurs during the peak negative cycle of the ultrasound pulse and the newly created microbubbles rapidly expand and collapse (Reznik et al. 2013; Sheeran et al. 2013a). Since vaporization of PSNE requires significantly higher pressures than what is used with traditional UCAs, the microbubbles are immediately subjected to high tensile stress that could lead to inertial cavitation. The short, high pressure pulses used in this study along with the detection of broadband emissions supports the theory of inertial cavitation as the main source of sonoporation.

Several studies have shown that inertial cavitation can sonoporate cells but often kills a large fraction of cells in the process (Sundaram et al. 2003; Hallow et al. 2006; Lai et al. 2006; Forbes et al. 2008). Acoustic cavitation induced cell lysis has a strong correlation with pulse length (Everbach et al. 1997; Brayman and Miller 1999; Chen et al. 2003b), which suggests that short pulses (< 10 cycles) may be more ideal for achieving reversible sonoporation. Sheeran *et al.* (2013a) showed that vaporized nanoemulsions are strongly affected by subsequent cycles after vaporization and undergo large amplitude oscillations and collapse that could cause extensive damage to cells. As shown in Figure 4, the viability of cells subjected to PSNE nucleated acoustic cavitation was indeed inversely related to pulse length. Based upon this finding, the shortest pulse length (*i.e.* five cycles) that ensured PSNE vaporization while minimizing cell death was selected for studies on siRNA delivery.

It has been suggested that the ratio between cavitation nuclei and cell concentration may be a critical factor in sonoporation (Guzman et al. 2003). Ward *et al.* (2000) hypothesized that increasing this ratio would reduce the bubble-to-cell distance significantly, thus increasing the likelihood of acoustic cavitation-induced membrane disruption. Additionally, studies using ultrasound contrast agents as cavitation nuclei have shown that quantified inertial cavitation activity is directly proportional to UCA concentration (Chen et al. 2003a; Hallow et al. 2006; Lai et al. 2006). We quantified inertial cavitation activity nucleated from PSNE and determined it had a logarithmic relationship with PSNE concentration (Figure 7E). This increase in inertial cavitation activity was accompanied by an increase in siRNA uptake by suspended cells (Figure 8). The fraction of suspended cells to which siRNA was delivered (*i.e.* sonoporation efficiency) was directly proportional to the concentration of PSNE and therefore the PSNE:cell ratio. Ratios ranged from 0.5 to 100, with significant (> 50%) uptake at PSNE:cell ratios of 25, 50, and 100. This finding is in good agreement with published results that show a similar relationship between sonoporation and UCA concentration (Miller and Quddus 2000; Lai et al. 2006; Karshafian et al. 2010). Unlike these published studies, however, cell viability was dramatically improved, remaining above 90% when measured via propidium iodide staining immediately following sonication. We

speculate that the high cell viability coupled with relatively efficient siRNA delivery (*i.e.* > 50% of initial cell population) was due to the use of very short pulses, which we showed previously was most ideal for minimizing cell death (Figure 4). Published sonoporation studies predominately have used pulse lengths longer than ten cycles, which unfortunately killed more cells (Lai et al. 2006; Karshafian et al. 2009). Cell viability differed depending on the metric used for quantification. Propidium iodide staining showed limited cell death immediately following treatment, while the cell proliferation assay showed a further reduction in viability measured at 24 hours after ultrasound exposure (Figure 4). We believe the proliferation assay takes into account all modes of cell death (irreparable cell membrane damage, apoptosis, cell fragmentation, etc.) and is more sensitive to how well the cells recover after the treatment.

In addition to the concentration of cavitation nuclei, we hypothesized that sonoporation efficiency depended strongly upon the duration of inertial cavitation activity. Studies have reported that inertial cavitation activity nucleated by UCAs disappeared within the first few seconds of ultrasound exposure (Hallow et al. 2006; Lai et al. 2006). This activity has also been reported in hemolysis experiments with UCAs, in which the authors describe a cascade effect of total microbubble destruction (Chen et al. 2003b). In our study, inertial cavitation nucleated by PSNE was sustained throughout the ultrasound exposure (Figure 7), thus increasing the probability of acoustic cavitation-induced cell membrane permeation and the resultant sonoporation efficiency. The sustained activity of PSNE may be explained by the higher concentrations of PSNE (10^9 vs. 10^7 per mL for UCAs) used in this study compared to previous sonoporation experiments. Since PSNE have a liquid core, high concentrations can be used without the acoustic shielding effects associated with high concentrations of gas-filled UCAs. These high concentrations in combination with the small focal volume used in this study may leave unvaporized PSNE outside the focal that can eventual propagate through and sustain cavitation activity.

Lastly, the sample volume relative to the transducer focal volume can have dramatic effects on acoustic cavitation-induced permeabilization of cell membranes. Assuming an ellipsoidal focal volume for the transducer used in this study, less than 1% of the total cell suspension volume lied within in the FWHM volume of the focus. The effect of this limited exposure volume can most clearly been seen in the heterogeneity of siRNA delivery, with subpopulations of cells showing uptake and no uptake. It is hypothesized that this effect is due to a large majority of the cell population not experiencing the same levels of acoustic cavitation induced stress. Some cells may never migrate through the focal volume of the transducer to interact with the microbubbles and others may experience different levels of permeation. The results from GFP siRNA delivery showed similar effects of heterogeneous delivery. A subpopulation of cells showed reduced levels of GFP indicated by their reduction in fluorescent intensity. This heterogeneity could be alleviated in future studies by mechanically translating the focus throughout the cell suspension or by actively mixing the suspension during treatment.

PSNE can be fabricated to have mean diameters that are small enough to take advantage of the EPR effect and accumulate in solid tumors (Rapoport et al. 2009; Kopechek et al. 2013; Williams et al. 2013). While studies have shown inconsistencies with the EPR effect due to

tumor heterogeneity, it is still a valuable way of targeting solid tumors with nanoparticles (Bae and Park 2011). Although free siRNA was used in this study, the functionality of a lipid shell allows addition of cationic or functional lipids that could be used to anchor the siRNA to the PSNE surface through electrostatic or covalent interactions. Previous ultrasound based siRNA delivery systems have used cholesterol-modified siRNA or cationic bubbles to complex the siRNA to the surface (Negishi et al. 2011; Endo-Takahashi et al. 2012). It is unknown whether the high PSNE:cell ratios and extracellular siRNA concentrations used in this *in vitro* study can be translated to *in vivo* scenarios. Modification of the surface properties and size of the PSNE might help penetration into tumors and interaction with target tumor cells. This would bring PSNE and siRNA closer to cells and therefore reduce the number of PSNE needed per cell.

Conclusions

Successful delivery of free siRNA to cancer cells with PSNE was achieved *in vitro* and was directly related to acoustic cavitation emissions. Our results indicate that with increasing PSNE-to-cell ratios, the amount of siRNA uptake and relative cavitation levels increased. This highlights the importance of bubble to cell interactions when invoking desired or undesired bioeffects caused by acoustic cavitation. PSNE displayed sustained acoustic cavitation levels throughout exposure durations and is unique compared to traditional UCAs. The ability to sustain acoustic cavitation activity could have a profound impact on other cavitation related therapies. In regards to PSNE as siRNA delivery vehicles, the amount of GFP knockdown in this study was similar to a commercial transfection agent. Due to the limitations of the ultrasound setup, heterogeneous knockdown was seen throughout the cell population and resulted in slightly lower levels of knockdown. Future work will focus on developing PSNE as siRNA carriers and explore differences between free siRNA delivery.

Acknowledgments

This work was supported in part by NIH grants R25CA153955 and R03EB015089.

References

Adan, MN.; Wilson, CG.; Fabiilli, ML.; Kripfgans, OD. Acoustic Droplet Vaporization-Induced Cellular Sonoporation. 2012 Ieee International Ultrasonics Symposium (Ius); 2012. p. 448-50.

Bae YH, Park K. Targeted drug delivery to tumors: myths, reality and possibility. J Control Release. 2011; 153:198–205. [PubMed: 21663778]

Behlke MA. Chemical modification of siRNAs for in vivo use. Oligonucleotides. 2008; 18:305–19. [PubMed: 19025401]

Brayman AA, Miller MW. Sonolysis of Albunex-supplemented, 40% hematocrit human erythrocytes by pulsed 1-MHz ultrasound: pulse number, pulse duration and exposure vessel rotation dependence. Ultrasound Med Biol. 1999; 25:307–14. [PubMed: 10320320]

Burnett JC, Rossi JJ, Tiemann K. Current progress of siRNA/shRNA therapeutics in clinical trials. Biotechnol J. 2011; 6:1130–46. [PubMed: 21744502]

Chen WS, Brayman AA, Matula TJ, Crum LA. Inertial cavitation dose and hemolysis produced in vitro with or without Optison. Ultrasound Med Biol. 2003a; 29:725–37. [PubMed: 12754072]

Chen WS, Brayman AA, Matula TJ, Crum LA, Miller MW. The pulse length-dependence of inertial cavitation dose and hemolysis. Ultrasound Med Biol. 2003b; 29:739–48. [PubMed: 12754073]

Davidson BL, McCray PB Jr. Current prospects for RNA interference-based therapies. Nat Rev Genet. 2011; 12:329–40. [PubMed: 21499294]

Elbashir SM, Harborth J, Lendeckel W, Yalcin A, Weber K, Tuschl T. Duplexes of 21-nucleotide RNAs mediate RNA interference in cultured mammalian cells. Nature. 2001; 411:494–8. [PubMed: 11373684]

Endo-Takahashi Y, Negishi Y, Kato Y, Suzuki R, Maruyama K, Aramaki Y. Efficient siRNA delivery using novel siRNA-loaded Bubble liposomes and ultrasound. Int J Pharm. 2012; 422:504–9. [PubMed: 22119963]

Everbach EC, Makin IR, Azadniv M, Meltzer RS. Correlation of ultrasound-induced hemolysis with cavitation detector output in vitro. Ultrasound Med Biol. 1997; 23:619–24. [PubMed: 9232771]

Fabiilli ML, Haworth KJ, Fakhri NH, Kripfgans OD, Carson PL, Fowlkes JB. The role of inertial cavitation in acoustic droplet vaporization. IEEE Trans Ultrason Ferroelectr Freq Control. 2009; 56:1006–17. [PubMed: 19473917]

Fan Z, Liu H, Mayer M, Deng CX. Spatiotemporally controlled single cell sonoporation. Proc Natl Acad Sci U S A. 2012; 109:16486–91. [PubMed: 23012425]

Fang J, Nakamura H, Maeda H. The EPR effect: Unique features of tumor blood vessels for drug delivery, factors involved, and limitations and augmentation of the effect. Adv Drug Deliv Rev. 2011; 63:136–51. [PubMed: 20441782]

Ferrara K, Pollard R, Borden M. Ultrasound microbubble contrast agents: fundamentals and application to gene and drug delivery. Annu Rev Biomed Eng. 2007; 9:415–47. [PubMed: 17651012]

Forbes MM, Steinberg RL, O'Brien WD Jr. Examination of inertial cavitation of Optison in producing sonoporation of chinese hamster ovary cells. Ultrasound Med Biol. 2008; 34:2009–18. [PubMed: 18692296]

Garg S, Thomas AA, Borden MA. The effect of lipid monolayer in-plane rigidity on in vivo microbubble circulation persistence. Biomaterials. 2013; 34:6862–70. [PubMed: 23787108]

Gilleron J, Querbes W, Zeigerer A, Borodovsky A, Marsico G, Schubert U, Manygoats K, Seifert S, Andree C, Stoter M, Epstein-Barash H, Zhang L, Koteliansky V, Fitzgerald K, Fava E, Bickle M, Kalaidzidis Y, Akinc A, Maier M, Zerial M. Image-based analysis of lipid nanoparticle-mediated siRNA delivery, intracellular trafficking and endosomal escape. Nat Biotechnol. 2013; 31:638–46. [PubMed: 23792630]

Guzman HR, McNamara AJ, Nguyen DX, Prausnitz MR. Bioeffects caused by changes in acoustic cavitation bubble density and cell concentration: a unified explanation based on cell-to-bubble ratio and blast radius. Ultrasound Med Biol. 2003; 29:1211–22. [PubMed: 12946524]

Guzman HR, Nguyen DX, Khan S, Prausnitz MR. Ultrasound-mediated disruption of cell membranes. II. Heterogeneous effects on cells. J Acoust Soc Am. 2001; 110:597–606. [PubMed: 11508985]

Hallow DM, Mahajan AD, McCutchen TE, Prausnitz MR. Measurement and correlation of acoustic cavitation with cellular bioeffects. Ultrasound Med Biol. 2006; 32:1111–22. [PubMed: 16829325]

Karshafian R, Bevan PD, Williams R, Samac S, Burns PN. Sonoporation by ultrasound-activated microbubble contrast agents: effect of acoustic exposure parameters on cell membrane permeability and cell viability. Ultrasound Med Biol. 2009; 35:847–60. [PubMed: 19110370]

Karshafian R, Samac S, Bevan PD, Burns PN. Microbubble mediated sonoporation of cells in suspension: clonogenic viability and influence of molecular size on uptake. Ultrasonics. 2010; 50:691–7. [PubMed: 20153497]

Kawabata K, Sugita N, Yoshikawa H, Azuma T, Umemura S. Nanoparticles with multiple perfluorocarbons for controllable ultrasonically induced phase shifting. Jpn J Appl Phys. 2005; 44:4548–52.

Kinoshita M, Hynynen K. A novel method for the intracellular delivery of siRNA using microbubble-enhanced focused ultrasound. Biochem Biophys Res Commun. 2005; 335:393–9. [PubMed: 16081042]

Kooiman K, Foppen-Harteveld M, van der Steen AF, de Jong N. Sonoporation of endothelial cells by vibrating targeted microbubbles. J Control Release. 2011; 154:35–41. [PubMed: 21514333]

Kopechek JA, Park E, Mei CS, McDannold NJ, Porter TM. Accumulation of phase-shift nanoemulsions to enhance MR-guided ultrasound-mediated tumor ablation in vivo. J Healthc Eng. 2013; 4:109–26. [PubMed: 23502252]

Kopechek JA, Zhang P, Burgess MT, Porter TM. Synthesis of phase-shift nanoemulsions with narrow size distributions for acoustic droplet vaporization and bubble-enhanced ultrasound-mediated ablation. J Vis Exp. 2012:e4308. [PubMed: 23007836]

Kripfgans OD, Fabiilli ML, Carson PL, Fowlkes JB. On the acoustic vaporization of micrometer-sized droplets. J Acoust Soc Am. 2004; 116:272–81. [PubMed: 15295987]

Kripfgans OD, Fowlkes JB, Miller DL, Eldevik OP, Carson PL. Acoustic droplet vaporization for therapeutic and diagnostic applications. Ultrasound Med Biol. 2000; 26:1177–89. [PubMed: 11053753]

Lai CY, Wu CH, Chen CC, Li PC. Quantitative relations of acoustic inertial cavitation with sonoporation and cell viability. Ultrasound Med Biol. 2006; 32:1931–41. [PubMed: 17169705]

Lares MR, Rossi JJ, Ouellet DL. RNAi and small interfering RNAs in human disease therapeutic applications. Trends Biotechnol. 2010; 28:570–9. [PubMed: 20833440]

Leighton, TG. The Acoustic Bubble. San Diego, California: Academic Press Inc; 1994.

Lentacker I, De Cock I, Deckers R, De Smedt SC, Moonen CT. Understanding ultrasound induced sonoporation: Definitions and underlying mechanisms. Adv Drug Deliv Rev. 2013

Liu Y, Yan J, Prausnitz MR. Can ultrasound enable efficient intracellular uptake of molecules? A retrospective literature review and analysis. Ultrasound Med Biol. 2012; 38:876–88. [PubMed: 22425381]

Miller DL, Quddus J. Sonoporation of monolayer cells by diagnostic ultrasound activation of contrast-agent gas bodies. Ultrasound Med Biol. 2000; 26:661–7. [PubMed: 10856630]

Negishi Y, Endo Y, Fukuyama T, Suzuki R, Takizawa T, Omata D, Maruyama K, Aramaki Y. Delivery of siRNA into the cytoplasm by liposomal bubbles and ultrasound. J Control Release. 2008; 132:124–30. [PubMed: 18804499]

Negishi Y, Endo-Takahashi Y, Ishii K, Suzuki R, Oguri Y, Murakami T, Maruyama K, Aramaki Y. Development of novel nucleic acid-loaded Bubble liposomes using cholesterol-conjugated siRNA. J Drug Target. 2011; 19:830–6. [PubMed: 21663557]

Neppiras EA. Acoustic cavitation Physics Reports (Review Section of Physics Letters). 1980; 61:159–251.

Ohl CD, Arora M, Ikink R, de Jong N, Versluis M, Delius M, Lohse D. Sonoporation from jetting cavitation bubbles. Biophys J. 2006; 91:4285–95. [PubMed: 16950843]

Phillips LC, Puett C, Sheeran PS, Wilson Miller G, Matsunaga TO, Dayton PA. Phase-shift perfluorocarbon agents enhance high intensity focused ultrasound thermal delivery with reduced near-field heating. J Acoust Soc Am. 2013; 134:1473–82. [PubMed: 23927187]

Rapoport NY, Kennedy AM, Shea JE, Scaife CL, Nam KH. Controlled and targeted tumor chemotherapy by ultrasound-activated nanoemulsions/microbubbles. J Control Release. 2009; 138:268–76. [PubMed: 19477208]

Reznik N, Shpak O, Gelderblom EC, Williams R, de Jong N, Versluis M, Burns PN. The efficiency and stability of bubble formation by acoustic vaporization of submicron perfluorocarbon droplets. Ultrasonics. 2013; 53:1368–76. [PubMed: 23652262]

Sheeran PS, Luois SH, Mullin LB, Matsunaga TO, Dayton PA. Design of ultrasonically-activatable nanoparticles using low boiling point perfluorocarbons. Biomaterials. 2012; 33:3262–9. [PubMed: 22289265]

Sheeran PS, Matsunaga TO, Dayton PA. Phase-transition thresholds and vaporization phenomena for ultrasound phase-change nanoemulsions assessed via high-speed optical microscopy. Phys Med Biol. 2013a; 58:4513–34. [PubMed: 23760161]

Sheeran PS, Streeter JE, Mullin LB, Matsunaga TO, Dayton PA. Toward ultrasound molecular imaging with phase-change contrast agents: an in vitro proof of principle. Ultrasound Med Biol. 2013b; 39:893–902. [PubMed: 23453380]

Sirsi SR, Borden MA. Advances in ultrasound mediated gene therapy using microbubble contrast agents. Theranostics. 2012; 2:1208–22. [PubMed: 23382777]

Sundaram J, Mellein BR, Mitragotri S. An experimental and theoretical analysis of ultrasound-induced permeabilization of cell membranes. Biophys J. 2003; 84:3087–101. [PubMed: 12719239]

Suzuki R, Oda Y, Utoguchi N, Maruyama K. Progress in the development of ultrasound-mediated gene delivery systems utilizing nano- and microbubbles. J Control Release. 2011; 149:36–41. [PubMed: 20470839]

Tokatlian T, Segura T. siRNA applications in nanomedicine. Wiley Interdiscip Rev Nanomed Nanobiotechnol. 2010; 2:305–15. [PubMed: 20135697]

Unger EC, Porter T, Culp W, Labell R, Matsunaga T, Zutshi R. Therapeutic applications of lipid-coated microbubbles. Adv Drug Deliv Rev. 2004; 56:1291–314. [PubMed: 15109770]

Vaishnaw AK, Gollob J, Gamba-Vitalo C, Hutabarat R, Sah D, Meyers R, de Fougerolles T, Maraganore J. A status report on RNAi therapeutics. Silence. 2010; 1:14. [PubMed: 20615220]

van Wamel A, Kooiman K, Harteveld M, Emmer M, ten Cate FJ, Versluis M, de Jong N. Vibrating microbubbles poking individual cells: drug transfer into cells via sonoporation. J Control Release. 2006; 112:149–55. [PubMed: 16556469]

Wang CH, Kang ST, Lee YH, Luo YL, Huang YF, Yeh CK. Aptamer-conjugated and drug-loaded acoustic droplets for ultrasound theranosis. Biomaterials. 2012; 33:1939–47. [PubMed: 22142768]

Ward M, Wu J, Chiu JF. Experimental study of the effects of Optison concentration on sonoporation in vitro. Ultrasound Med Biol. 2000; 26:1169–75. [PubMed: 11053752]

Whitehead KA, Langer R, Anderson DG. Knocking down barriers: advances in siRNA delivery. Nat Rev Drug Discov. 2009; 8:129–38. [PubMed: 19180106]

Williams R, Wright C, Cherin E, Reznik N, Lee M, Gorelikov I, Foster FS, Matsuura N, Burns PN. Characterization of submicron phase-change perfluorocarbon droplets for extravascular ultrasound imaging of cancer. Ultrasound Med Biol. 2013; 39:475–89. [PubMed: 23312960]

Wu J, Nyborg WL. Ultrasound, cavitation bubbles and their interaction with cells. Adv Drug Deliv Rev. 2008; 60:1103–16. [PubMed: 18468716]

Wu SY, Lopez-Berestein G, Calin GA, Sood AK. RNAi therapies: drugging the undruggable. Sci Transl Med. 2014; 6:240ps7.

Zhang P, Porter T. An in vitro study of a phase-shift nanoemulsion: a potential nucleation agent for bubble-enhanced HIFU tumor ablation. Ultrasound Med Biol. 2010; 36:1856–66. [PubMed: 20888685]

Zhang S, Zhao B, Jiang H, Wang B, Ma B. Cationic lipids and polymers mediated vectors for delivery of siRNA. J Control Release. 2007; 123:1–10. [PubMed: 17716771]

Zhou Y, Yang K, Cui J, Ye JY, Deng CX. Controlled permeation of cell membrane by single bubble acoustic cavitation. J Control Release. 2012; 157:103–11. [PubMed: 21945682]

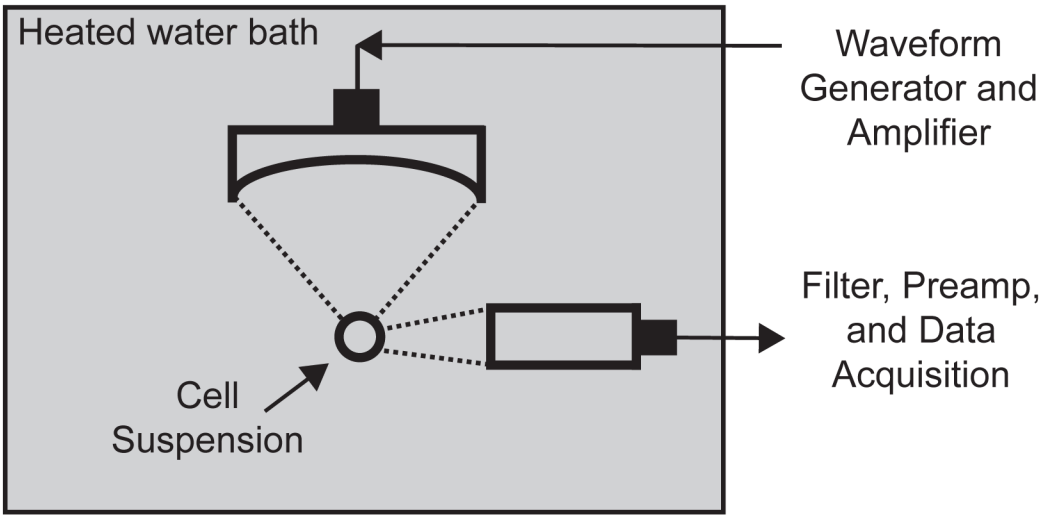

Figure 1.

Schematic of the experimental set-up for small interfering RNA (siRNA) delivery to a cell suspension using phase-shift nanoemulsions (PSNE). A 5 MHz focused ultrasound transducer was used to sonicate cells suspended in a microcentrifuge tube. Acoustic cavitation emissions were detected throughout the ultrasound exposure using an unfocused passive cavitation detector (PCD) and quantified to test correlation with siRNA uptake.

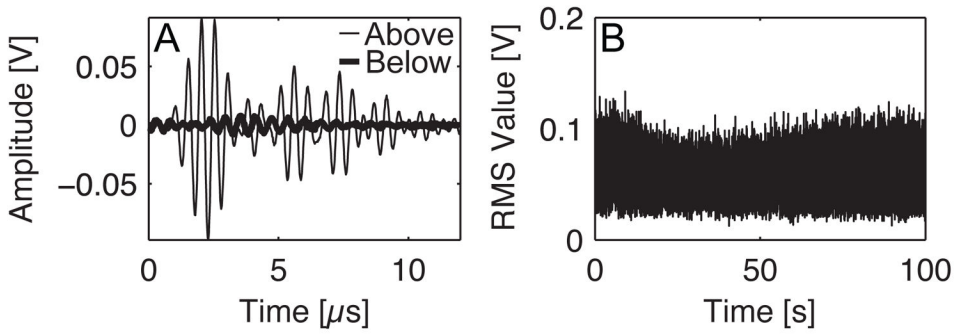

Figure 2.

Method for quantification of acoustic cavitation activity during ultrasound exposures using phase-shift nanoemulsions (PSNE) as cavitation nuclei for small interfering RNA (siRNA) delivery to cells by sonoporation. (A) Individual traces were recorded throughout the exposure duration resulting in approximately 25,000 traces per exposure (5 cycle pulses, 250 Hz pulse repetition frequency, 100 second treatment duration, 6.2 MPa peak negative pressure, and n=3 at each PSNE concentration). The above plot depicts traces that were recorded above and below the pressure threshold for PSNE vaporization. (B) The root mean square (RMS) value was taken of each individual trace and plotted versus exposure time to give a trend of cavitation activity. In order to provide a quantitative measure of the cavitation activity, the RMS values were summated over exposure time to produce a single value that represents the amount of cavitation activity for a given exposure. These values were then normalized to the exposure with the highest amount of cavitation activity for comparison between different exposures. This provides a relative metric of cavitation activity for correlation with siRNA uptake and cell viability. Lastly, the mean and standard deviations were taken for all exposure groups at different PSNE concentrations (5×10^6, 1×10^7, 2.5×10^7, 5×10^7, 1×10^8, 2.5×10^8, 5×10^8, and 1×10^9 PSNE/mL).

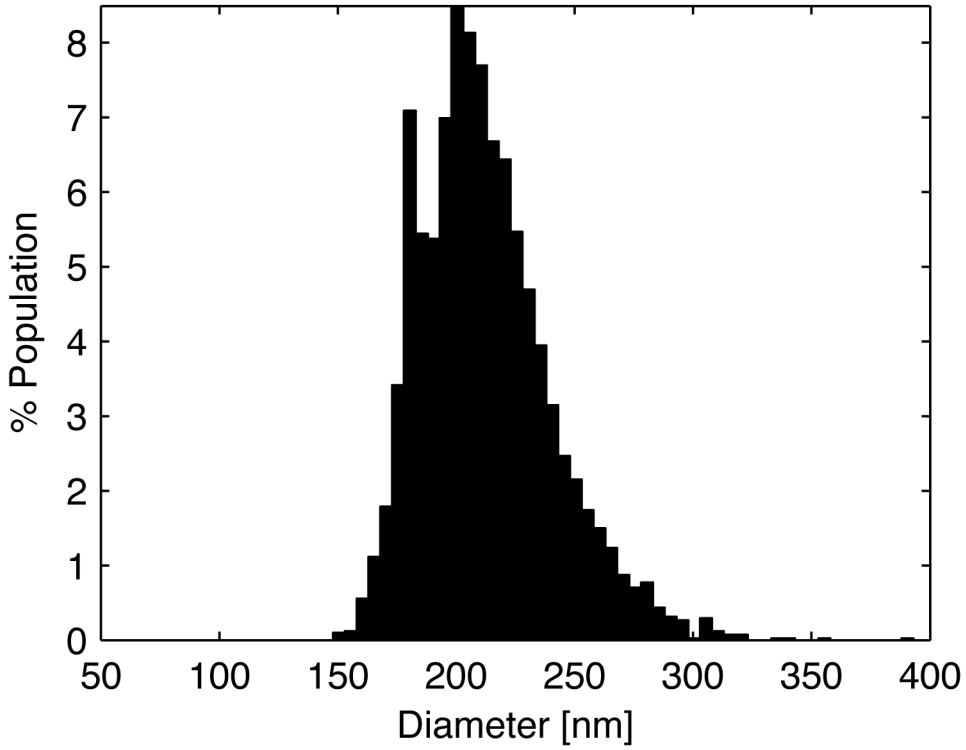

Figure 3.

Size distribution measurements of phase-shift nanoemulsions (PSNE) using tunable resistive pulse sensing with the qNano instrument. PSNE had a mean diameter of 213 nm (31.4 standard deviation) and a modal diameter of 203 nm (+/− 2.2). The d50, d10, and d90 values were 208.7 nm, 180.1 nm, and 250.4 respectively with a d90/d10 value of 1.4 and a span of 0.3.

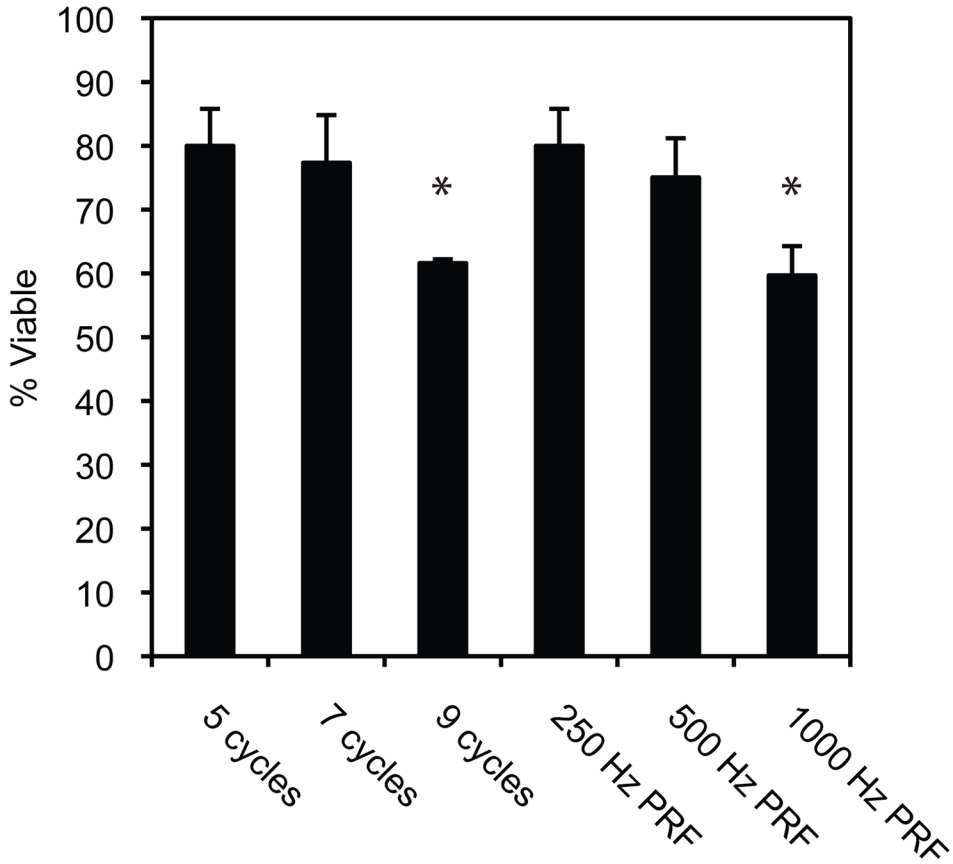

Figure 4.

Cell viability dependence on pulse length and pulse repetition frequency (PRF). Cell proliferation assays were performed 24 hours post ultrasound exposures at varying pulse lengths (5, 7, and 9 cycles) at a fixed PRF (250 Hz) and varying PRFs (250, 500, and 1000 Hz) at a fixed number of cycles (5 cycles). The total treatment time was 100 seconds with a peak negative pressure of 6.2 MPa. Data is expressed as the mean +/− the standard deviation (n=3, *p<0.05 versus 5 cycle, 250 Hz PRF treatment).

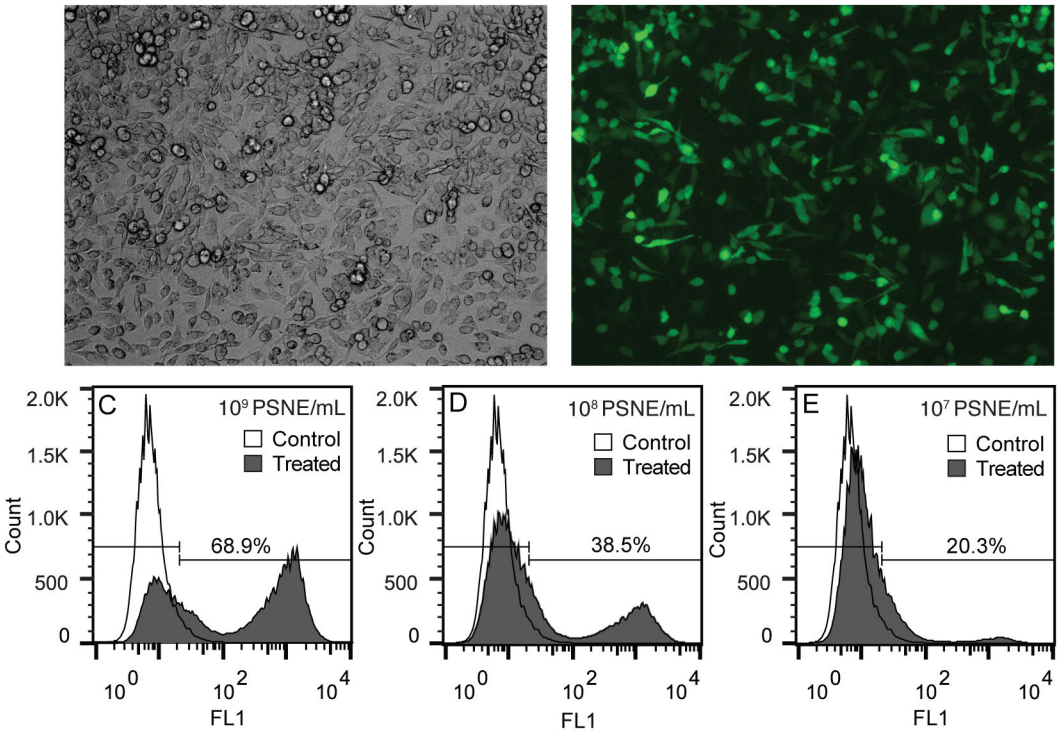

Figure 5.

Representative fluorescent microscopy and flow cytometry results from fluorescent small interfering RNA (siRNA) delivery experiments with phase-shift nanoemulsions (PSNE). (A) Brightfield and (B) fluorescent microscopy images of cells cultured for eight hours after ultrasound exposure testing the uptake of siRNA tagged with a green fluorophore. Flow cytometer results of siRNA uptake at (C) 1×10^9, (D) 1×10^8, and (E) 1×10^7 PSNE/mL are shown in the bottom three histograms. Cells showing uptake of siRNA were gated using the FL1 (green) fluorescent intensity channel of the flow cytometer. The ultrasound parameters used were 5 cycle pulses, 250 Hz pulse repetition frequency, 100 second treatment duration, and a peak negative pressure of 6.2 MPa.

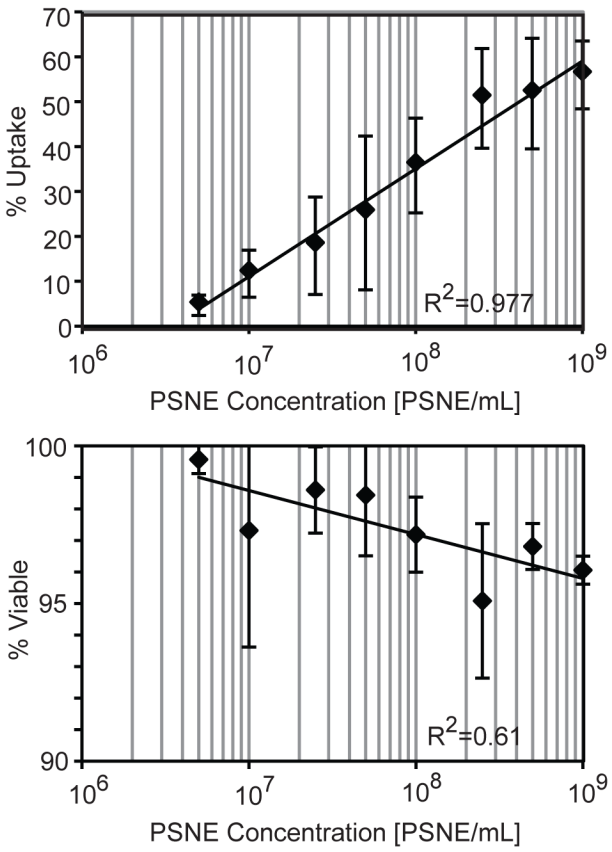

Figure 6.

The effect of phase-shift nanoemulsion (PSNE) concentration on siRNA uptake and cell viability. The x-axis is on a logarithmic scale and logarithmic trendlines were used to fit the data. The ultrasound parameters used were 5 cycle pulses, 250 Hz pulse repetition frequency, 100 second treatment duration, and a peak negative pressure of 6.2 MPa.

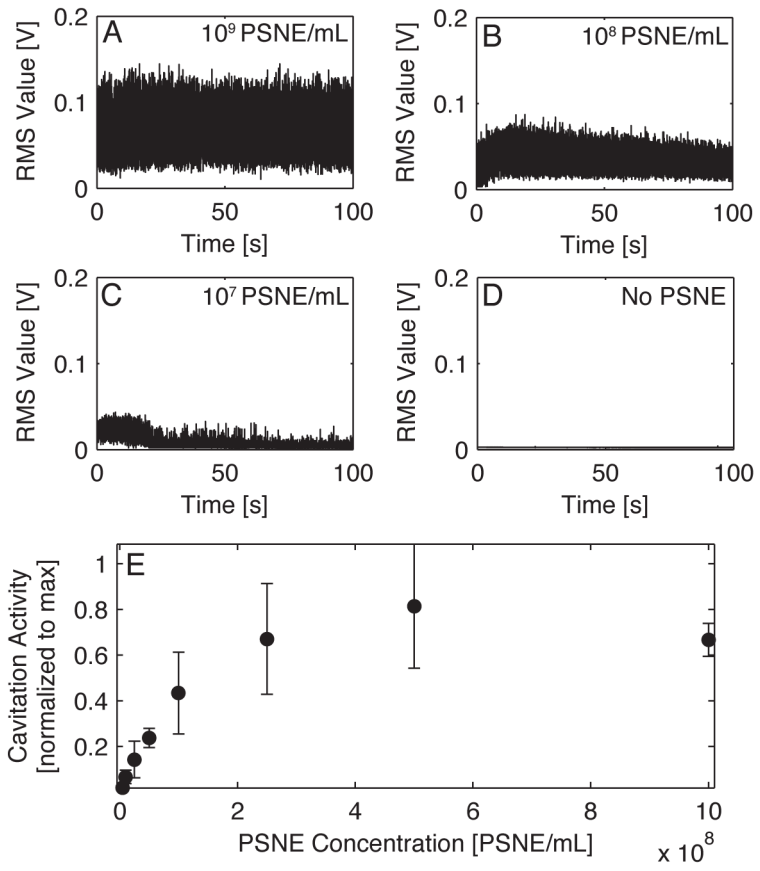

Figure 7.

Example plots of the root mean square (RMS) values of cavitation activity versus exposure time for treatments at (A) 1×10^9 PSNE/mL, (B) 1×10^8 PSNE/mL, (C) 1×10^7 PSNE/mL and (D) no PSNE. (E) The mean normalized cavitation activity value plotted versus phase-shift nanoemulsion (PSNE) concentration. The ultrasound parameters used were 5 cycle pulses, 250 Hz pulse repetition frequency, 100 second treatment duration, and a peak negative pressure of 6.2 MPa.

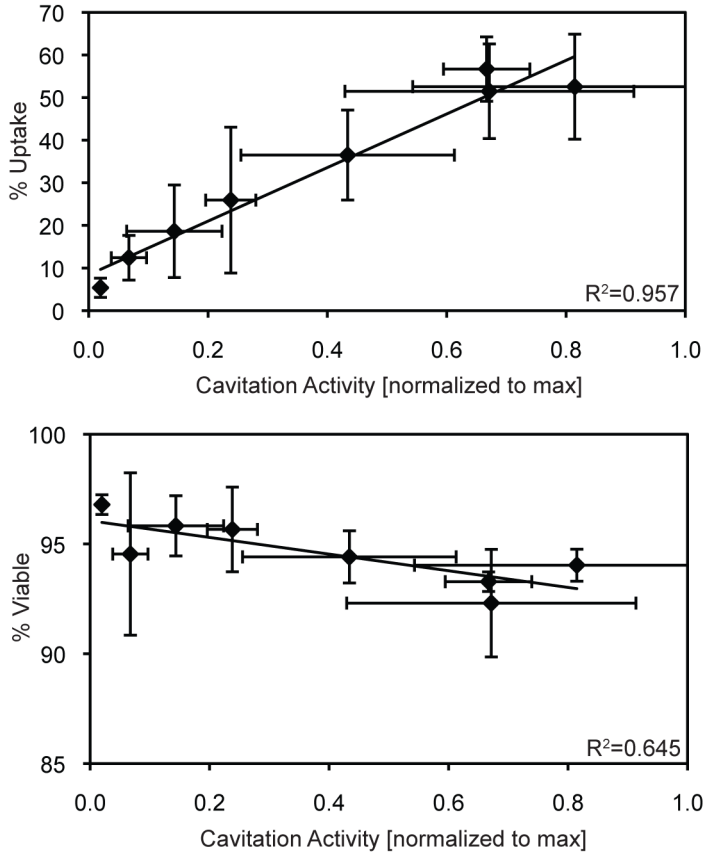

Figure 8.

Correlation of cavitation activity with small interfering RNA (siRNA) uptake and cell viability. The means +/− the standard deviations (n=3) were plotted and linear trendlines were used to fit the data. The ultrasound parameters used were 5 cycle pulses, 250 Hz pulse repetition frequency, 100 second treatment duration, and a peak negative pressure of 6.2 MPa.

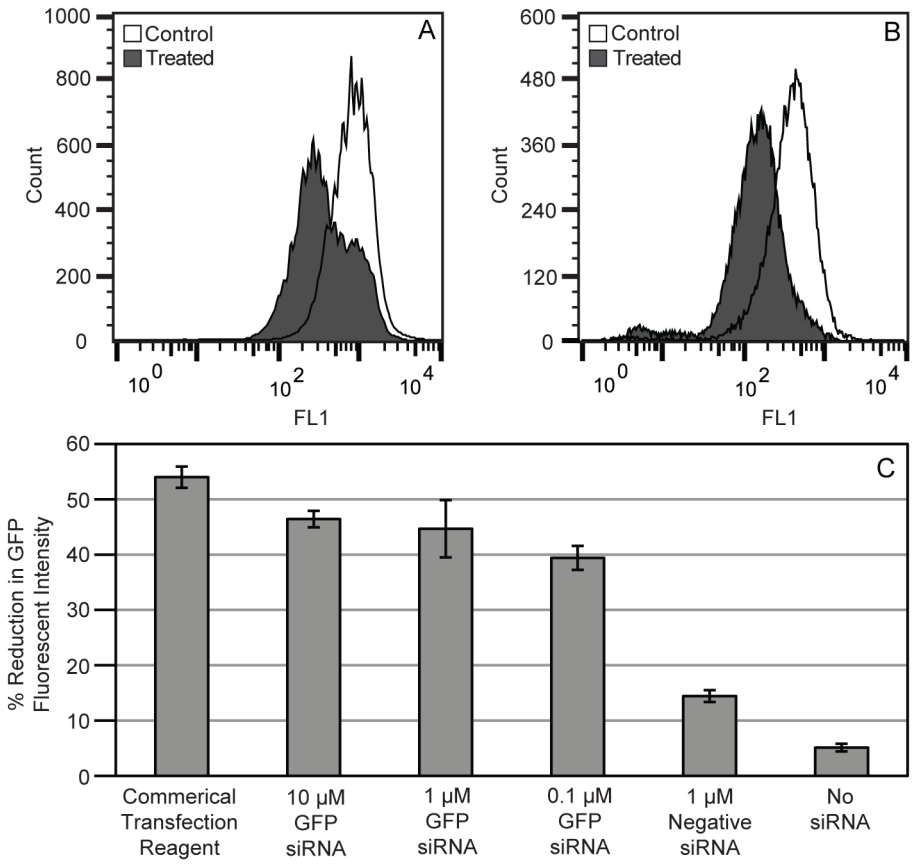

Figure 9.

Results from treatments using green fluorescent protein (GFP) targeted small interfering RNA (siRNA). Flow cytometer histogram results using a (A) commercial transfection agent and (B) acoustic cavitation mediated delivery with PSNE. The histograms depict treated and control cell populations with a treated cells showing decreased levels of GFP fluorescent intensity 48 hours post ultrasound treatment. (C) The bar plots show the overall reduction of GFP fluorescent intensity at various concentrations of GFP siRNA (10 μM, 1 μM, and 0.1 μM) and controls (commercial transfection agent, negative siRNA, and no siRNA). The ultrasound parameters used were 5 cycle pulses, 250 Hz pulse repetition frequency, 100 second treatment duration, and a peak negative pressure of 6.2 MPa.